Chemical Engineering & Processing: Process Intensification 179 (2022) 109093

Contents lists available at ScienceDirect

Chemical Engineering and Processing - Process Intensification

journal homepage: www.elsevier.com/locate/cep

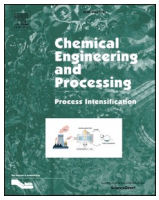

Performance analysis of biomass gasification coupled with ultra-supercritical power generation system

Haolin Liu [a], Chao Ye [a,*], Yuan Zhao [b], Guoneng Li [a], Yousheng Xu [a], Yuanjun Tang [a], Guanqun Luo [a], Qinhui Wang [c,*]

[a] Department of Energy and Environmental System Engineering, Zhejiang University of Science and Technology, Hangzhou, Zhejiang 310023, China
[b] Powerchina HuaDong Engineering Corporation Limited, Hangzhou 311122, China
[c] State Key Laboratory of Clean Energy Utilization, Zhejiang University, Hangzhou, Zhejiang 310027, China

ARTICLE INFO

Keywords:
Biomass gasification
Coal-fired power plant
Energy and exergy efficiency
Pollutant emissions
CO_2 reduction

ABSTRACT

In order to alleviate the impact of coal combustion on the environment, a scheme of biomass gasification in coal-fired ultra-supercritical power plant is proposed and simulated with Aspen plus. Simulation results show that the energy and exergy efficiencies of the coupled system have an increasing-decreasing tendency with the increase of the air/biomass ratio, reaching the maximum value when the air/biomass ratio is 1.6. The energy and exergy efficiencies of the coupled system decrease continuously with the increase of the excess air ratio. The coupled system has the highest energy and exergy efficiencies of 46.89% and 43.13%, which are 2.70% and 1.81% higher than those of an ultra-supercritical coal-fired system, respectively. Meanwhile, the coupled system has low CO_2, SO_2, and NO_x emissions and thus many advantages in terms of environmental performance.

1. Introduction

Coal accounted for more than half of China's primary energy consumption and will still have an important role for a long time [1–3]. Coal is mainly used for electricity production through the steam Rankine Cycle. Despite the rapid development of renewable energy, including nuclear, wind and biomass energy in recent years, the share of thermal power generation (mainly from coal- fired power) of China more than 60% in the past years [1,4,5]. At the United Nations General Assembly in 2020, China clearly proposed to strive for the peak of carbon dioxide emissions before 2030 and strive to achieve carbon neutrality before 2060. CO_2 emission reduction is not only a basic requirement for China to achieve scientific development [6,7], but also a strategic measure for the international community to cope with climate change [8,9]. In terms of the existing coal utilization technologies, the utilization efficiency must be improved, and the coal consumption must be decreased.

According to the steam Rankine cycle, the efficiency of power generation is generally improved by increasing the parameters of steam, including pressure and temperature. Coal-fired power generation technology is developing significantly from subcritical power generation technology to ultra-supercritical power generation technology after decades of development [10]. Generally, the steam parameters of power plants exceed 24 MPa and 600 °C, which characterize ultra-supercritical power generation technology. The steam parameters of the latest ultra-supercritical power generation technology have exceeded 25 MPa/600 °C and will reach 30 MPa and 700 °C in years to come [11]. According to the literature, the power generation efficiency of newly built ultra-supercritical power plants can reach more than 45% [12,13]. Compared with subcritical and supercritical power generation technologies, the coal utilization efficiency of ultra-supercritical power generation technology is significantly increased. Thus, coal consumption can be reduced, and the reduction of CO_2 emissions can be achieved simultaneously when ultra-critical power generation technology is extensively used. To explore the market feasibility, Vu et al. conducted a techno-economic analysis of ultra-supercritical power plants using air- and oxy-combustion CFB with and without CO_2 capture, and the net efficiency of the oxy-combustion power plant is higher (39%) and cost of electricity is lower (59 $/MWh) [13]. Rocha and Silva performed exergy-environmental analysis on an 800 MWe coal-fired power plant adopting ultra-supercritical technology [14].

Given the increasing urgency of the demand for CO_2 emissions reduction, the China National Energy Administration and the Ministry of Ecology and Environment issued "A notice about the construction of biomass coal-coupled power generation pilot project" in 2017. The

* Corresponding authors.
E-mail addresses: 118065@zust.edu.cn (C. Ye), qhwang@zju.edu.cn (Q. Wang).

https://doi.org/10.1016/j.cep.2022.109093
Received 27 April 2022; Received in revised form 1 August 2022; Accepted 5 August 2022
Available online 7 August 2022

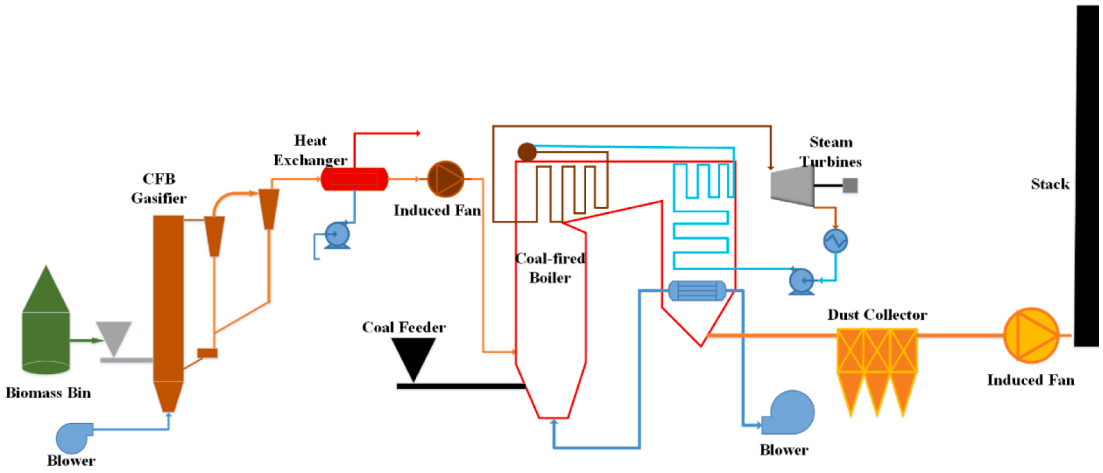

Fig. 1. Diagram of biomass gasification coupled with ultra-supercritical power plant system.

technology mentioned in the document aims to prompt the R&D of biomass utilization technology in commercial operational conventional coal-fired power stations to further reduce coal consumption and CO_2 emissions. At present, biomass is mainly applied in biomass direct-fire power plants [15], with some disadvantages. First, biomass is difficult to utilize in large scale because of the dispersed distribution of biomass resources and seasonal variation [16,8]. Second, high-parameter steam is difficult to produce because of the high-temperature corrosion and fouling of heating surfaces. Therefore, developing biomass gasification in coal-fired power plants is becoming increasingly important resolving the existing problems. This system can be realized by adding a CFB gasifier based on the coal-fired power plant and the syngas produced from biomass gasification instead of sending the biomass itself to the boiler for combustion. The gasification temperature is much lower than that of direct biomass combustion, preventing the melted AAEMs from fouling the heating surfaces. Compared with the biomass direct-combustion system, the combination of biomass gasification and coal combustion is beneficial for producing high-parameter steam. Meanwhile, the separation of biomass gasification and coal combustion will minimize the impacts of integration on the existing coal-fired system.

Few studies related to the coupled system exist. Zhang et al. proposed the integration of corn straw gasification in a coal-fired power generation station which merits our further consideration [17]. They performed performance analysis on the power generation system under various loads. However, only the boiler efficiency and the pollutants emission were calculated, and the characteristics of this system were not fully demonstrated.

In our article, the coupling of biomass gasification with a 600-MW ultra-supercritical power generation system is proposed, with corn straw as the feedstock of the gasifier. The combination of biomass utilization and ultra-supercritical power generation technology aims to realize the reduce CO_2 and other pollutant emissions under the premise of ensuring the efficiency of power generation. The effects of the air/biomass ratio and the excess air coefficient for combustion on the system performance are studied. The results of biomass gasification are compared with the experimental results to verify the feasibility of the simulation results. Then, thermodynamic and pollutants emissions analyses are conducted, and the results are compared with those of an ultra-supercritical coal-fired power plant. This study aims to provide data references for the commercial operation of coupled power generation in the future.

Table 1
Proximate and ultimate analysis of corn straw and coal.

Fuel		Corn Straw	Coal
Proximate analysis(wt%)	Fixed Carbon	17.75	46.39
	Volatile Matter	71.45	25.12
	Ash	5.93	20.94
	Moisture	4.87	7.55
Ultimate analysis(wt%)	Carbon	44.56	61.14
	Hydrogen	5.33	3.18
	Oxygen	38.45	12.95
	Nitrogen	0.74	1.23
	Sulfur	0.12	0.56
Lower heating value (MJ/kg)		16.29	21.93

2. Material and methods

2.1. System description

The coupled power generation system is mainly composed of biomass gasification unit and coal-fired power plant unit, as shown in Fig. 1. The preheated corn straws and western China coal is employed as the simulation material and the proximate and ultimate analysis are listed in Table 1. Corn straws are gasified with air in the CFB gasifier to generate syngas. The mass flowrate of feeding biomass 72 t/h. The operational temperature of gasification is between 700 °C and 800 °C. The syngas is sent to heat exchanger after leaving the gasifier. In the heat exchanger, the syngas is cooled to approximately 400 °C. The cooled syngas is fed to the coal-fired boiler and combusted with pulverized coal. The combustion temperature is between 1200 °C and 1400 °C [18]. The flue gas passes through the tail heating surface and high-parameter steam are generated. The parameters of steam are 28.2 MPa/600 °C/620 °C. Finally, high-parameter steam is sent to steam turbines for power generation. After working in steam turbines, exhausted steam is cooled in the condenser and flows into deaerator where mix with feedwater. Then, the feedwater is preheated in the preheater. The regenerative cycle uses low-pressure heaters and high-pressure heaters. The preheated water goes through the boiler and becomes high-parameter steam again.

2.2. System modeling

The simulation study of coupled system is accomplished by Aspen Plus which is a widely employed in coal conversion industry and shows well applicability by existing studies [19,20]. PR-BM model is applied in the simulation of coupled system, which is applicable for calculating the physical and chemical exergy of both liquid and gas phases in all streams

Table 2
The nomenclature in the article.

Abbreviation	Full name
CFB	Circulated Fluidized Bed
AAEM	Alkali and Alkaline Earth Metals
PR-BM	Peng-Robinson with Boston-Mathias
HPHs	high-pressure heaters
LPHs	low-pressure heaters
HPTs	high-pressure turbines
IPTs	intermediate pressure turbines
LPTs	low-pressure turbines
LHV	Lower heating value

based on the second law of thermodynamics.

The abbreviations of nouns and their full names in the article are listed in Table 2.

2.2.1. Biomass gasification coupled with pulverized coal combustion unit

The biomass gasification or pulverized coal combustion is divided into two steps, including pyrolysis, gasification and combustion [21], respectively. In the pyrolysis process, the volatile in the coal is devolatilized and coal or biomass is decomposed into gas and char. In the gasification or combustion process, homogeneous reactions and heterogenous reactions occur between the gas and char. All of the above reactions are listed in the following part [19].

$$2C + O_2 \rightarrow 2CO \quad (1)$$

$$C + O_2 \rightarrow CO_2 \quad (2)$$

$$C + H_2O \rightarrow CO + H_2 \quad (3)$$

$$H_2 + O_2 \rightarrow H_2O \quad (4)$$

$$C + CO_2 \rightarrow 2CO \quad (5)$$

$$CO + H_2O \rightarrow CO_2 + H_2 \quad (6)$$

$$C + 2H_2 \rightarrow CH_4 \quad (7)$$

$$C + 2H_2O \rightarrow CO_2 + 2H_2 \quad (8)$$

According to the conversion characteristics of biomass and coal, there are two steps during the simulation of biomass gasification and coal combustion, including decomposition process and reaction process. Firstly, the gas component such as H_2, O_2, N_2, CO, H_2O, and CO_2 are defined as conventional components, while biomass, coal, and ash are defined as unconventional components [22]. Secondly, the Ryield model is adopted to simulate the decomposition process where fuel breaks up into C, H_2, O_2, N_2, S, H_2O, and ash [23]. The elements yields are calculated by the built-in Fortran module based on the proximate and ultimate analysis of biomass and coal. Thirdly, the elements from Ryield model are sent to Rigibbs model which models the reaction process, in which the elements interact with each other. The Rigibbs model is based on the mechanism of Gibbs free energy minimization. In the meantime, part of the heat from biomass gasification and coal combustion flow to biomass pyrolysis reactor for and coal pyrolysis reactor, and the other is set as heat loss. The heat loss value is 3% of the lower heating value of biomass and coal.

2.2.2. Steam power cycle unit

The steam power cycle unit mainly consists of steam turbines, heaters, and pumps and is shown in Fig. 2 [4]. Liquid water is compressed to 28.2 MPa before the feed water enters the boiler. Three high-pressure heaters (HPHs) and three low-pressure heaters (LPHs) are used, and the feed water is heated to approximately 380 °C. Then, the water flows into the ultra-supercritical boiler and goes through the heating surfaces distributed around the furnace. The water is heated to ultra-supercritical condition by dramatic heat exchange with the high-temperature gas generated by the intense chemical reactions [14]. Then, the high-parameter steam is sent to the high-pressure turbines (HPTs) and works after expansion. Part of exhaust steam from the HPTs is transferred to the HPHs for water heating, and the other steam is sent back to the boiler for reheating to raise the steam conditions. The reheating steam (620 °C/4.5 MPa) feeds the intermediate pressure turbines (IPTs), and two steam extractions are directed to the HPH-2 and HPH-3, and part of exhaust steam of IPT is directed to the deaerator. The remaining steam is sent to the low-pressure turbines (LPTs) after leaving the IPTs and works in the LPTs. In the LPTs, three steam extractions are directed to the LPHs, and the remaining steam goes to the condenser for cooling. The condensed water exchanges heat with the external water in the condenser [24]. Then, the feed water leaving the condenser passes through the water preheaters (i.e., HPHs, LPHs, and deaerator).

2.3. Performance analysis

Several parameters are introduced to evaluate the thermodynamic performance of biomass coupled ultra-supercritical power generation system.

$$E_{COAL} = LHV_{COAL} \cdot m_{COAL} \quad E_{BIOMASS} = LHV_{BIOMASS} \cdot m_{BIOMASS} \quad (10)$$

Where E_{COAL}(MW) and $E_{BIOMASS}$(MW) represent the total heating value of coal and biomass, LHV_{COAL}(MJ /kg) and $LHV_{BIOMASS}$(MJ /kg) represent the lower heating value of coal and coal, and m_{COAL}(kg /s) and $m_{BIOMASS}$(kg /s) represent the mass flowrate of feed coal.

$$E_{SYNGAS} = LHV_{H2} \cdot V_{H2} + LHV_{CO} \cdot V_{CO} + LHV_{CH4} \cdot V_{CH4} \quad (11)$$

Where E_{SYNGAS}(MW) means the total heating value of syngas,

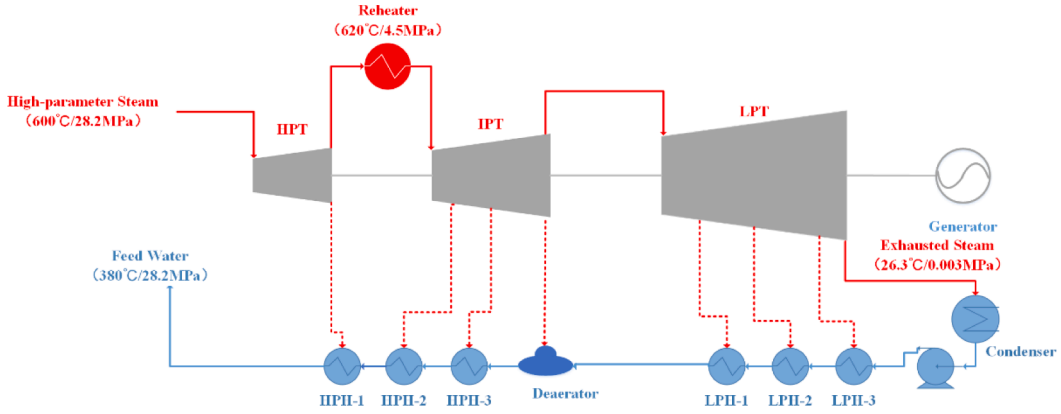

Fig. 2. Steam power cycle unit.

Table 3
The input parameters of coupled system.

Parameters	1	2	3	4	5
Biomass input (kg/s)	20	20	20	20	20
Coal input (kg/s)	43	43	43	43	43
Air input for biomass gasification (kg/s)	24	28	32	36	40
Air/biomass ratio (kg/kg)	1.2	1.4	1.6	1.8	2.0
Air input for combustion (kg/s)	519	519	519	519	519

$LHV_{H2}(MJ/Nm^3)$, $LHV_{CO}(MJ/Nm^3)$, and $LHV_{CH4}(MJ/Nm^3)$ means the lower heating value of H_2, CO, and CH_4, and $V_{H2}(Nm^3/s)$ represents the volume flow rate of H_2, CO, and CH_4.

$$\eta_t = E/(E_{COAL} + E_{BIOMASS})\cdot 100\% \quad (12)$$

Where $\eta_t(\%)$ represents the energy efficiency of coupled system and E(MW) represents the power generation of coupled system.

$$E = E_{total} - E_{pumps} - E_{fans} \quad (13)$$

Where E_{pumps} represents power consumption of pumps and E_{fans} represents the power consumption of fan.

$$EX = EX_{ph} + EX_{ch} \quad (14)$$

Where EX(MW) denotes the total exergy, $EX_{ph}(MW)$ denotes the physical exergy, and $EX_{CH}(MW)$ denotes the chemical exergy.

The physical exergy and chemical exergy can be calculated by Eqs. (14) and (15) [2,25]:

$$EX_{ph} = (h_i - h_o) - T_0(S_i - S_o) \quad (15)$$

$$EX_{ch} = \sum x_i EX_{ch}^0 + RT_0 \sum x_i \ln(x_i) \quad (16)$$

The chemical exergy of multiple components gas is obtained based on the standard value of each component [26].

The exergy efficiency of subsystem can be expressed by the following equations [27].

$$\varepsilon_i = (EX_{i,in} - EX_{i,out})/EX_{i,in} * 100\% \quad (17)$$

Where $\varepsilon_i(\%)$ represents the exergy efficiency of subsystem, $EX_{i,in}(MW)$ represents the exergy flow that enters the subsystem and $EX_{i,out}(MW)$ represents the exergy flow that leaves the subsystem. The i means the subsystem of gasifier, combustor and steam turbines.

The exergy value of the input coal and biomass is acquired by calculation methods proposed by Szargut and Styrylska [28,29]

$$EX = LHV\cdot\left(1.0438 + 0.0013\cdot\frac{H}{C} + 0.1083\cdot\frac{O}{C} + 0.0549\cdot\frac{N}{C}\right) + 6.17\cdot s \quad (18)$$

Where C, H, O, N and S represent the mass fraction of carbon, hydrogen, oxygen, nitrogen and sulfur.

$$\varepsilon = EX_{ELECTRICITY}/(EX_{COAL} + EX_{BIOMASS})\cdot 100\% \quad (19)$$

Where $\varepsilon(\%)$ represents the exergy efficiency of coupled system, $EX_{EIECTRICITY}(MW)$ represents the exergy of power generation, and $EX_{COAL}(MW)$ and $EX_{BIOMASS}(MW)$represent the exergy of coal and biomass, respectively.

$$\eta_{gas} = LHV_{syn}\times(V_{syn} - V_{H2O}) \times 22.4/3600/(20 \times 16.9) \quad (20)$$

Where LHV_{syn} represents the lower heating value of syngas, V represents the volume of syngas and H_2O (kmol/h).

3. Results and discussions

3.1. The effects of air/biomass ratio on system performance

The air/biomass ratio is directly related to the gasification characteristics, including but not limited to the gasification temperature, the gasification efficiency, and the syngas components [30,31]. Furthermore, the gasification characteristics have a significant effect on the coupled system performance. Five working conditions are simulated in this study, and the input parameters of the five runs are listed in Table 3. The simulation results based on the input parameters are shown in Figs. 3 and 4.

Fig. 3 indicates that the gasification temperature continuously increases as the air/biomass ratio varies from 1.2 to 2. Becasuse more air input results in R (2) (4) (9) intensified and more heat is released. According to Fig. 4, the volume fractions of H_2 and CH_4 keeps decreasing as the air/biomass ratio increases, while the volume fraction of CO shows an increasing–decreasing trend. The above conclusions are consistent with the expermental results in the existing literature [32]. Because as more air input, R(1) is intensified and more carbon is converted to CO, which makes less carbon used for R (3). The produced H_2 is less than consumed H_2 which makes H_2 content decrease. R (7) is weakened with H_2 content decreasing, and CH_4 content decreases. The volume of gas in gasification and the integral number of synthetic gas are listed in Table 4. With the variation of the syngas components, the lower heating value of syngas presents an increasing–decreasing trend. When the air/biomass ratio is 1.4, the lower heating value of syngas has a maxium value of 6.0 MJ/Nm^3. When the air/biomass ratio is more than 1.4, the

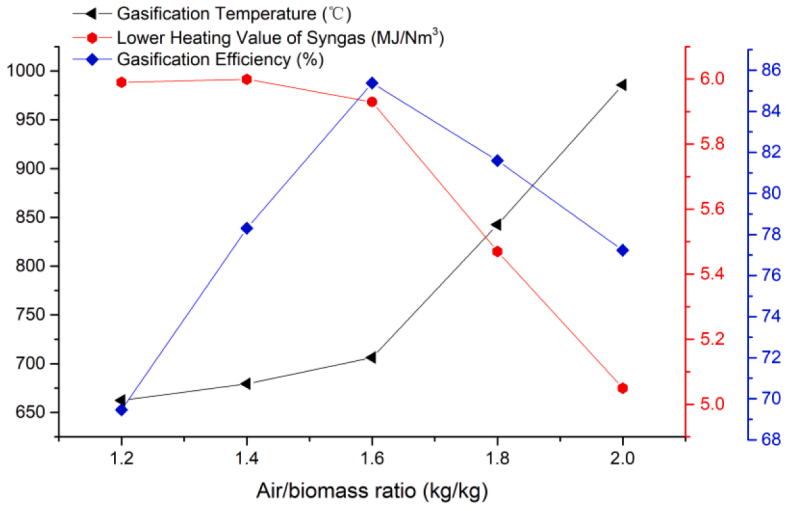

Fig. 3. The effect of air/biomass ratio on gasification characteristics.

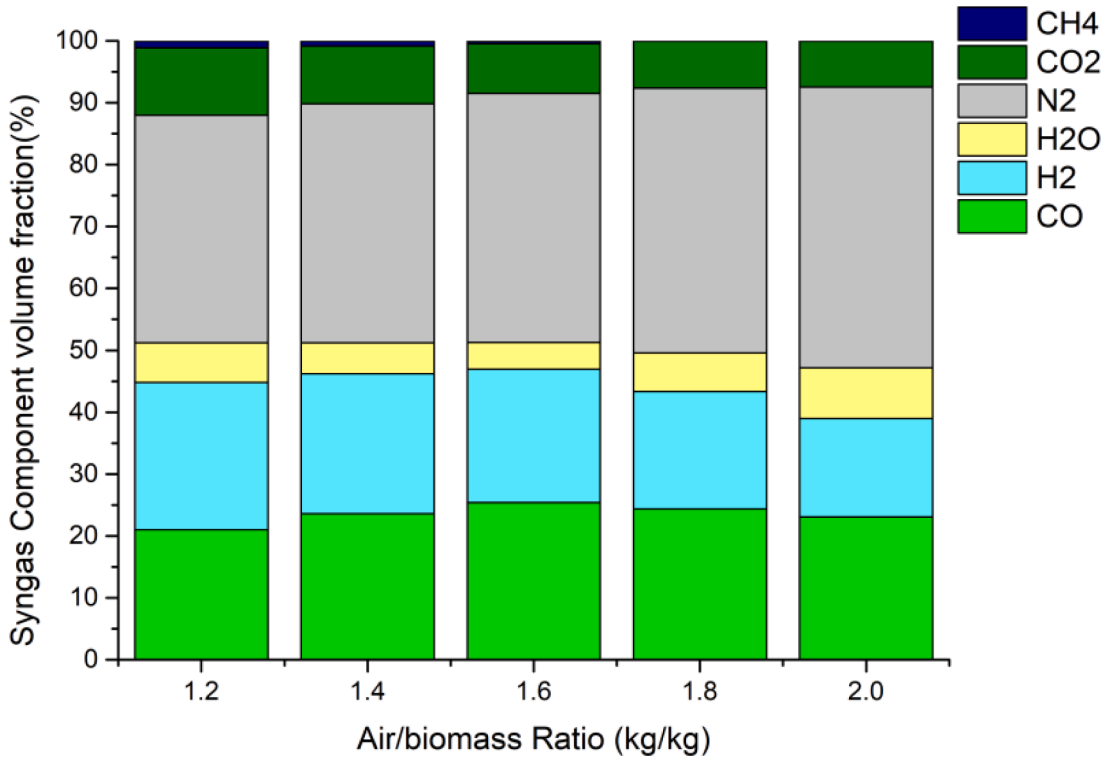

Fig. 4. The effect of air/biomass ratio on syngas components.

Table 4
The effect of air biomass ratio on gas parameters.

Air/Biomass Ratio	Gas		LHV	Temperature
1.2	Total volume	6484.52		1139.74
	Gas volume fraction			
	CO	20.98	12.64	
	H_2	23.83	10.79	
	CH_4	1.07	35.88	
	syngas	45.88	5.99	
1.4	Total volume	7191.45		1174.47
	Gas volume fraction			
	CO	23.58		
	H_2	22.6		
	CH_4	0.79		
	syngas	46.97	6.00	
1.6	Total volume	7879.284		1202.48
	Gas volume fraction			
	CO	25.4		
	H_2	21.54		
	CH_4	0.39		
	syngas	47.33	5.93	
1.8	Total volume	7879.284		1196.37
	Gas volume fraction			
	CO	24.39		
	H_2	18.93		
	CH_4	0.0059		
	syngas	43.3259	5.47	
2.0	Total volume	8334.18		1192.75
	Gas volume fraction			
	CO	25.4		
	H_2	21.54		
	CH_4	0.39		
	syngas	47.33	5.04	

lower heating value decreases rapidly. When the air/biomass ratio is 1.6, the volume fraction of H_2O in the gas is the lowest, only 4.32%, and the volume fraction of CO and CH_4 reaches the peak, so the syngas under the conditions has high lower heating value and the highest gasification efficiency. The gasification efficiency increases iniatially to its peak vlue of 85.38% and then decreased. At the initial stage of the increase of air volume, the reaction R(1) and R(2) can be guaranteed. At the same time, the increased temperature can make R(3) and R(5) proceed in the direction of positive reaction. However, when the air volume continues to increase, R(4) and R(9) will become the main reaction process, and the consumption of CO and H_2 will increase.

Table 5
The effect of air biomass ratio on energy production / consumption.

Air/Biomass ratio	1.2	1.4	1.6	1.8	2
Etotal	581.54	599.78	615.05	614.9	614.73
Epumps	8.79	9	9.18	9.18	9.18
Efans	10.81	10.87	10.95	11.03	11.11
E	561.94	579.91	594.92	594.69	594.44

Equivalence ratio is an important parameter in the process of biomass gasification, which is expressed as the ratio of air demand for gasification to air demand for complete combustion. When the equivalence ratio is 0.25~0.30, the gas composition produced by gasification is ideal. The air demand for complete combustion of corn straw is calculated by (21), where [C]=44.56%, [H]=5.33%, [O]=38.45%.

$$V = 1.866[C] + 5.55[H] + 0.7[S] - 0.7[O] \quad (21)$$

After calculation, it can be seen that the total combustion air volume of corn straw is 4.11 m^3/kg. The input of biomass is 20 kg, and the air required for complete combustion is 82.20 m^3, equivalent to 106.04 kg. The equivalence ratio is 0.25~0.30, and the amount of air required for gasification is 26.51~31.81 kg. At this time, the air biomass ratio is 1.33~1.59. Therefore, when the air biomass ratio is 1.6, the maximum gasification efficiency is achieved.

In terms of system efficiency, the energy efficiency, the exergy efficiency, and the power generation have an increasing–decreasing tendency as the air/biomass ratio increases. They increase significantly and then declines slightly. The effect of air biomass ratio on energy production/consumption is listed in Table 5. The energy consumption of pumps and fans would gradually increase with the increase of air

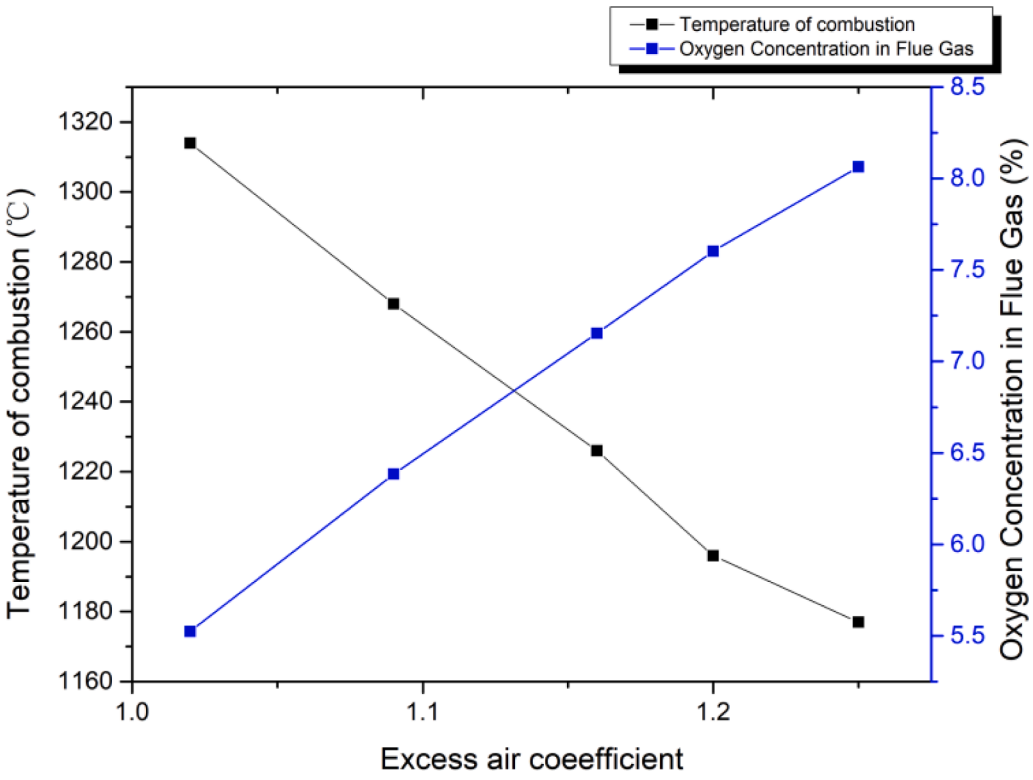

Fig. 5. The effect of air coefficient on temperature of combustion and oxygen concentration in flue gas.

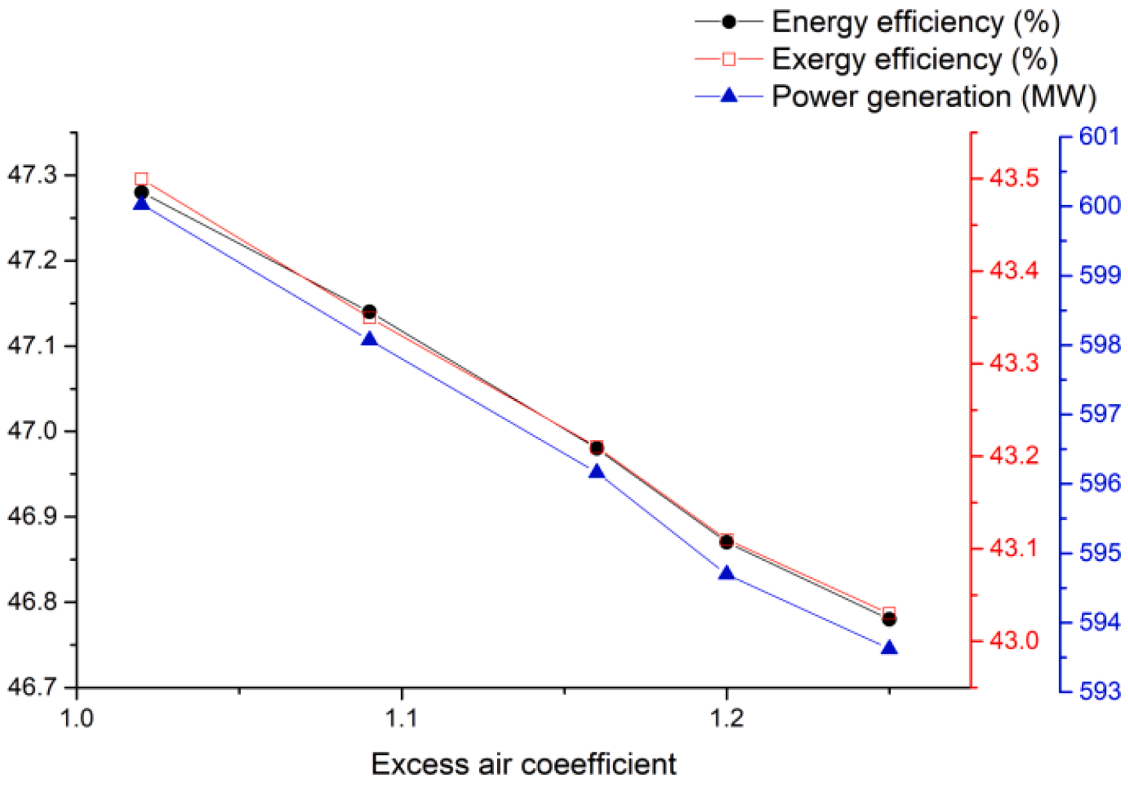

Fig. 6. The effect of excess air coefficient on energy efficiency and exergy efficiency.

biomass ratio, but the total power generation will reach the maximum when the ratio is 1.6. After further calculation, when the air/biomass ratio is 1.6, the energy efficiency, the exergy efficiency, and the power generation reach the maximum values of 46.89%, 43.13%, and 594.92 MW, respectively.

Table 6
The input parameters of coupled system.

Parameters	1	2	3	4	5
Biomass input (kg/s)	20	20	20	20	20
Coal input (kg/s)	43	43	43	43	43
Air input for biomass gasification (kg/s)	32	32	32	32	32
Air/biomass ratio (kg/kg)	1.6	1.6	1.6	1.6	1.6
Air input for combustion (kg/s)	440	470	500	519	540

Table 7
The simulation results of biomass gasification under determined air/biomass ratio.

Items	Simulated Value	Experimental Value [30]
Volume fraction of syngas components(%)		
H_2	22.44	17.3
CO	26.45	22.6
CO_2	8.33	12.0
N_2	41.94	45.7
CH_4	0.41	1.98
Lower heating value of syngas (MJ/Nm^3)	5.93	5.70
Syngas yield(Nm^3/kg)	2.45	/
Gasification temperature(°C)	706	/
Gasification efficiency(%)	85.38	/

3.2. The effects of excess air coeffcient on system performance

According to the optimum air/biomass ratio of 1.6, the system performance under different excess air coefficients is shown in Figs. 5 and 6. The loss caused by incomplete combustion needs to be considered. The loss of incomplete combustion in biomass gasification is taken as 2%, while the loss of incomplete combustion in coal-fired boilers is taken as 5.5%. The operational parameters of the five runs are listed in Table 6, and the simulation results of biomass gasification are listed in Table 7. Under the determined operating parameter, the temperature of biomass gasification is 706 °C, and the gasification efficiency is 85.38%. The syngas yield is 2.45 Nm^3/kg, and the lower heating value is 5.93 MJ/Nm^3. The simulated results are compared with the experimental results of biomass gasification to prove the feasibility of the biomass gasification model. Table 7 shows that the volume fractions of CO and H_2 are higher than those of the referenced results [30]. Meanwhile, the volume fractions of CO_2, N_2, and CO_2 are smaller than those of the experimental results because the simulated gasification process is nearer the ideal condition, which is based on the minimum Gibbs free energy priciple. The Boudouard reaction has a thorough process, which leads to increased CO production and decreased CO_2 production [17]. Meanwhile, the Methanation reaction is weakened because of the increased C consumption, which results in increased H_2 production and decreased CH_4 production [17]. The explanations above indicate that the simulation model of biomass gasification can be validated by the experimental results.

Fig. 5 shows that combustion temperature decreases from 1314 °C to 1177 °C when the excess air cofficient increases. This phenomenon can be attributed to the existence of a theoretical air quantity for a certain combustion condition. When the air quantity exceeds the theoretical air quantity, the excess air does not participate in the combustion reactions. Meanwhile, the excess would absorb the heat from the combustion reaction, decreasing the combustion temperature. The oxygen concentration in flue gas decreases continuously when the excess air coefficient increases because the excess oxygen is improved simutaneously. Fig. 6 indicates that both energy and exery efficiencies decrease continuously when the excess air coefficient increases from 1.02 to 1.25 because the power generation decreases from 618.62 MW to 614.15 MW. Therefore, raising the excess air coefficient is not conducive to the improvement of system efficiency.

Table 8
Input parameters and material flows for exergy calculation.

Parameters	Value	
Biomass input (kg/s)	20	
Coal input (kg/s)	43	
Air input for biomass gasification (kg/s)	32	
Air/biomass ratio (kg/kg)	1.6	
Air input for combustion (kg/s)	519	
Excess air coefficient	1.2	
Component	Mass flowrate of syngas(kg/h)	Mass flowrate of flue gas(kg/h)
H_2	3422.29	/
O_2	/	179206
N_2	88894.73	1534920
CO	56049.81	2.96
CO_2	27839.57	381761
CH_4	493.30	/
C_2H_4	0.0028	/
C_3H_6	$1.65{\cdot}10^{-10}$	/
C_3H_8	$4.08{\cdot}10^{-8}$	/
C_2H_6	0.0025	/
NH_3	5.73	/
SO_2	$1.13{\cdot}10^{-6}$	1489.37
SO_3	$2.99{\cdot}10^{-17}$	21.42
H_2S	86.59	$1.34{\cdot\cdot}10^{-11}$
COS	8.83	/
H_2O	6140.18	81518.19
NO	$9.63{\cdot}10^{-11}$	1513.92
NO_2	$1.82{\cdot}10^{-22}$	7.65
Total	182941	2180440
Temperature(°C)	706	1202

3.3. Exergy analysis of the coupled system

In this section, one operational condition is determined, and the parameters and the material flows are listed in Table 8. Exergy analysis is performed on each part to explore the distribution of exergy destruction, and the exergy value of each part is presented in Fig. 7. The coupled system has three main subsystems, namely, the biomass gasifier, the coal and syngas combustor, and the steam turbines.

As is shown in Fig. 7, the exergy efficiency of the coal and syngas combustor is the lowest (i.e., 39.8%). The exergtic destruction is nearly 60%. The combustor has two main exergy destruction [33], namely, the irreversible dissipation of fuel combustion and the exergetic destruction of heating exchangers, because the high-quality energy (chemical energy) is converted to low-quality energy (heat), which is used for steam generation. Consequently, a relatively large exergetic destruction is obtained [34]. The exergy efficiency of the biomass gasifier is 76.39%, which is higher than that of the combustor. Unlike the combustor, the biomass in the gasifer is converted to syngas instead of flue gas. Table 8 shows that syngas is rich in CO and H_2 and has a high chemical energy. Among the three subsystems, the steam turbines have the highest exergy efficiency of 86.59%.

3.4. Performance and emissions comparison of coupled system and ultra-supercritical coal-fired power plant

This section proposes an ultra-supercritical coal-fired power plant whose performance is compared with that of the coupled system. The input parameters and simulation results of the ultra-supercritical coal-fired power plant and the coupled system are listed in Table 9.

In this section, the two systems use the same coal, and the coal mass flow rates of the two systems are 43 and 60.5 kg/s, respectively. The mass flowrate of biomass for the coupled system is 20 kg/s. The air/biomass ratio is 1.6, and the excess air coefficients for two systems are very close, namely, 1.2 and 1.18, respectively. The combustion temperature of the two systems is the same (i.e., 1202 °C), and the parameters of power generation are 600 °C/620 °C/28.2 MPa.

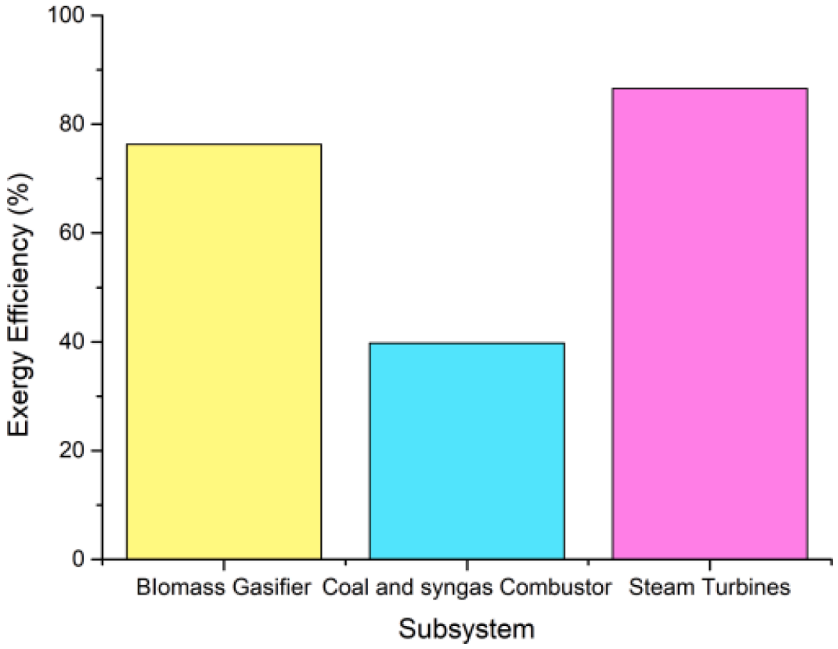

Fig. 7. Exery efficiency of subsystem of coupled system.

Table 9
Performance and emissions comparison of coupled system and ultra-supercritical coal-fired power plant.

Items	Biomass gasification coupled coal-fired power plant	Ultra-critical coal-fired power plant
Input		
Biomass input(kg/s)	20	/
Coal input (kg/s)	43	60.5
Air input for biomass gasification(kg/s)	32	/
Air input for coal combustion(kg/s)	519	545
Air/biomass ratio(kg/kg)	1.6	/
Excess air coefficient	1.2	1.18
Combustion temperature (°C)	1202	1202
Parameters of power generation	600 °C/620 °C/28.2 MPa	600°C/620 °C/28.2 MPa
Output		
Total power generation (MW)	615.05	606.19
Total power consumption (MW)	20.13	19.94
Gross power generation (MW)	594.92	586.73
Energy efficiency(%)	46.89	44.19
Exergy efficiency(%)	43.13	41.32
CO_2 emissions(kg/KW·h) Before purification	0.83	0.58
NO_x emissions(mg/Nm^3) Before purification	648.91	658.15
SO_2 emissions(mg/Nm^3)- Before purification	635.17	809.13

Under the determined input parameters, the total power generation values of the two systems are 615.05 MWand 606.19 MW, respectively. Considering the power consumption, the gross power generation values are 594.92 MWand 586.73 MW, respectively, because determining which scheme is better based on the power generation is difficult. The energy and exergy efficiencies of the two systems are calculated. The energy and exergy efficiencies of the coupled system are 46.89% and 43.13%, respectively. The energy and exergy efficiencies of the ultra-supercritical coal-fired power plant are 44.19% and 41.32%, respectively, indicating that both the energy and exergy efficiencies of the coupled system are higher than those of the coal-fired power plant, which means that the coupled system has advantages over the existing coal-fired power plant.

The pollutant emissions are not only related to the normal operation of power plants but also to sustainable economic and social development. Therefore, the pollutant emissions of the two systems must be compared. The sulfur and nitrogen contents in coal, biomass, and air are converted into hazardous air pollutants, inlcuding SO_2, NO, and NO_2. All of the air pollutants are harmful to ecology and human health. The lastest emission standards for coal-fired power plants are 35 mg/Nm^3 for SO_2 and 50 mg/Nm^3 for NO_x, which are the strictest emission standards in history [35]. Therefore, the vast majority of air pollutants should be removed before being discharged into the atmosphere, which need numbers of cost consumption. Limestone-gypsum wet FGD and SCR denitration are the most widely applied end-of-pipe treatment processes in removing SO_2 and NO_x[36,37]. However, 1 kg of SO_2 emission reduction is estimated to be accompanied by an extra generation of 4.64 kg CO_2 and 0.016 kg NO_x. Meanwhile, 1 kg of NO_x emission reduction is accompanied by an extra generation of 1.88 kg CO_2 and 0.008 kg SO_2 [38]. The current flue gas purification measures entail large costs and result in extra pollutants and CO_2. Therefore, novel pollutant reduction technologies should be developed urgently, and the reduction of coal combustion should be enhanced on the source.

Table 9 indicates that the SO_2 and NO_x emissions of the coal-fired power plant are 809.13 and 658.16 mg/Nm^3, respectively, while the SO_2 and NO_x emissions of the coulped system are 635.17 and 648.91 mg/Nm^3, respectively. Furthermore, 173.93- and 9.24-mg/Nm^3 NO_x reductions can be achieved in the biomass gasification coupling with the coal-fired power system. The SO_2 emission can be decreased by more than 20% because the SO_2 formation is mainly from the reactions of the sulfur content in biomass and coal with oxygen. Meanwhile, the sulfur content in biomass is much smaller than that in coal, resulting in less SO_2 formation. NO_x is mainly composed of the majority of NO and a small part of NO_2. NO formation is mainly related to the combustion temperature and the N_2 in air of which the differences are much less while in coal-fired power plant and coupled system [39]. Therefore, the difference in NO_x emissions is small. In general, the coupling of biomass gasification and the coal-fired power system can effectively reduce SO_2 and NO_x emissions and flue gas purification costs.

Table 9 clearly shows that the CO_2 emission in the coupled system is much lower than that in the coal-fired power plant. The CO_2 emissions in the coal-fired power plant and the coupled system is 0.83 and 0.58 kg/kW·h, respectively, indicating that the biomass gasification coupled system reduces the CO_2 emission by more than 30%, and the emission reduction effect is very effective.

4. Conclusion

In this study, the coupling of biomass gasification and the ultra-supercritical coal-fired system is simulated. Several important parameters of the coupled system are researched under different air/biomass ratios and excess air coefficients. Meanwhile, the simulations results are compared with those of the ultra-supercritical coal-fired power plant, resulting in the following conclusions:

(1) The air/biomass ratio has an influence on the performance of biomass gasification and power generation. When the air/biomass ratio is 1.6, the gasification, energy, and exergy efficiencies reach the maximum values of 85.35%, 46.89%, and 43.13%, respectively.
(2) The energy and exergy efficiencies of the coupled system decrease continuously with the increase of the excess air coefficient.
(3) The coupling of biomass gasification and the ultra-supercritical coal-fire system has higher energy and exergy efficiencies and lower CO_2, SO_2, and NO_x emissions than the conventional coal-fired ultra-supercritical power plant.
(4) Biomass gasification and pulverized coal combustion technologies can be organically combined and become a high-efficiency and low-CO_2 and -pollutants emissions technology.

Credit author statement

1 This article research results are reported by the person from all of the original research achievements, paper contains no others have been published or has been written but not yet published research results, without any infringement of others or other problems of the copyright owner of intellectual property rights.
2 This article contains no political errors, nor does it involve any state secrets or any sensitive issues unsuitable for publication.
3 The research results reported in this paper (including all or part of the data in the figure and table) have not been published or submitted to other scientific journals; All or part of this paper will not be submitted to other journals before receiving the notice of disposal of manuscripts from Energy.
4 The author of this paper has learned about the stance and practice of CARBON against the author's two submissions for a paper or two submissions for a paper in a different form and the infringement of others' intellectual property rights.
5 The author acknowledges the importance of the commitments embodied in this statement and accepts all consequences arising from any breach of such commitments.

CRediT authorship contribution statement

Haolin Liu: Investigation, Methodology, Writing – original draft. **Chao Ye:** Conceptualization, Methodology, Funding acquisition, Writing – review & editing. **Yuan Zhao:** Writing – review & editing. **Guoneng Li:** Writing – review & editing. **Yousheng Xu:** Writing – review & editing. **Yuanjun Tang:** Writing – review & editing. **Guanqun Luo:** Writing – review & editing. **Qinhui Wang:** Writing – review & editing.

Declaration of Competing Interest

The authors declare that they have no known competing financial interests or personal relationships that could have appeared to influence the work reported in this paper.

Data availability

No data was used for the research described in the article.

Acknowledgments

The work is supported by Zhejiang Provincial Natural Science Foundation of China under Grant (No. LQ21E060002) (No. LQ21E0600001) and National Science Foundation of China (11972324) (51906220) (5200060864).

References

[1] Q. Wang, China Energy Data of 2019 (2019).
[2] C. Ye, Y. Zheng, Y. Xu, G. Li, C. Dong, Y. Tang, Q. Wang, Energy and exergy analysis of poly-generation system of hydrogen and electricity via coal partial gasification, Comput. Chem. Eng. (2020), 106911.
[3] C. Ye, Z. Ye, Z. Zhu, Q. Wang, Thermodynamic and economic analysis of Oxy-Fuel-Integrated coal partial gasification combined cycle, ACS Omega 6 (6) (2021) 4262–4272.
[4] Y. Liu, Q. Li, X. Duan, Y. Zhang, Z. Yang, D. Che, Thermodynamic analysis of a modified system for a 1000 MW single reheat ultra-supercritical thermal power plant, Energy 145 (2018) 25–37.
[5] Y. Tang, J. Dong, G. Li, Y. Zheng, Y. Chi, A. Nzihou, E. Weiss-Hortala, C. Ye, Environmental and exergetic life cycle assessment of incineration- and gasification-based waste to energy systems in China, Energy 205 (2020), 118002.
[6] F. Chu, M. Su, G. Yang, Heat and mass transfer characteristics of ammonia regeneration in packed column, Appl. Therm. Eng. 176 (2020), 115405.
[7] F. Chu, G. Xiao, G. Yang, Mass transfer characteristics and energy penalty analysis of MEA regeneration process in packed column, Sustain. Energy Fuels 5 (2) (2021) 438–448.
[8] H. Liu, C. Ye, Y. Xu, Q. Wang, Effect of activation conditions and iron loading content on the catalytic cracking of toluene by biochar, Energy 247 (2022), 123409.
[9] Q. Wang, C. Ye, Y. Zhao, H. Liu, Y. Tang, G. Luo, W. Guo, C. Dong, G. Li, Y. Xu, Preparation of Polydopamine-Derived Carbon-Based Nano-Fe Catalysts and its Catalytic Conversion of Toluene for Hydrogen Production, Soc. Sci. Electr. Publ. (2022).
[10] J. Bugge, S. Kjær, R. Blum, High-efficiency coal-fired power plants development and perspectives, Energy 31 (10-11) (2006) 1437–1445.
[11] F. Sun, Y.F. Gu, J.B. Yan, Y.X. Xu, Z.H. Zhong, M. Yuyama, Creep deformation and rupture mechanism of an advanced wrought Ni Fe-based superalloy for 700°C class A-USC steam turbine rotor application, J. Alloys Compd. 687 (2016) 389–401.
[12] X. Lin, Q. Li, L. Wang, Y. Guo, Y. Liu, Thermo-economic analysis of typical thermal systems and corresponding novel system for a 1000 MW single reheat ultra-supercritical thermal power plant, Energy 201 (2020), 117560.
[13] T.T. Vu, Y.I. Lim, D. Song, T.Y. Mun, J.H. Moon, D. Sun, Y.T. Hwang, J.G. Lee, Y. C. Park, Techno-economic analysis of ultra-supercritical power plants using air- and oxy-combustion circulating fluidized bed with and without CO_2 capture, Energy 194 (2020), 116855.
[14] D.H.D. Rocha, R.J. Silva, Exergoenvironmental analysis of a ultra-supercritical coal-fired power plant, J. Clean. Prod. 231 (2019) 671–682.
[15] L. Yan, Z. Wang, Y. Cao, B. He, Comparative evaluation of two biomass direct-fired power plants with carbon capture and sequestration, Renew. Energy 147 (2020) 1188–1198.
[16] B. Yang, Y.M. Wei, Y. Hou, H. Li, P. Wang, Life cycle environmental impact assessment of fuel mix-based biomass co-firing plants with CO_2 capture and storage, Appl. Energy 252 (2019), 113483.
[17] X. Zhang, K. Li, C. Zhang, A. Wang, Performance analysis of biomass gasification coupled with a coal-fired boiler system at various loads, Waste Manag. 105 (2020) 84–91.
[18] J. Zhou, P. Ling, S. Su, J. Xu, K. Xu, Y. Wang, S. Hu, M. Zhu, J. Xiang, Exergy analysis of a 1000 MW single reheat advanced supercritical carbon dioxide coal-fired partial flow power plant, Fuel 255 (2019), 115777.
[19] C. Ye, Q. Wang, Y. Zheng, G. Li, Z. Zhang, Z. Luo, Techno-economic analysis of methanol and electricity poly-generation system based on coal partial gasification, Energy 185 (2019) 624–632.
[20] R. Tavares, E. Monteiro, F. Tabet, A. Rouboa, Numerical investigation of optimum operating conditions for syngas and hydrogen production from biomass gasification using Aspen Plus, Renew. Energy 146 (2020) 1309–1314.
[21] C. Ye, Q. Wang, Z. Luo, M. Fang, K. Cen, Techno-economic analysis of novel power generation system based on coal partial gasification technology, Asia-Pac. J. Chem. Eng. 14 (6) (2019) e2377.

[22] W. Lan, G. Chen, X. Zhu, X. Wang, C. Liu, B. Xu, Biomass gasification-gas turbine combustion for power generation system model based on ASPEN PLUS, Sci. Total Environ. 628-629 (2018) 1278–1286.
[23] B. Liu, X. Yang, W. Song, W. Lin, Process simulation development of coal combustion in a circulating fluidized bed combustor based on Aspen Plus, Energy Fuels 25 (4) (2011) 1721–1730.
[24] L. Xiao, M. Yang, W.-Z. Yuan, S.-M. Huang, Coupled heat and mass transfer of cross-flow random hollow fiber membrane tube bundle used for seawater desalination, Int. J. Heat Mass Transf. 152 (2020), 119499.
[25] I. Dincer, M.A. Rosen, Exergy: Energy, Environment and Sustainable Development, Newnes, 2012.
[26] T.J. Kotas, The Exergy Method of Thermal Plant Analysis, Elsevier, 2013.
[27] Y. Zhao, M. Liu, C. Wang, Z. Wang, D. Chong, J. Yan, Exergy analysis of the regulating measures of operational flexibility in supercritical coal-fired power plants during transient processes, Appl. Energy 253 (2019), 113487.
[28] G. Zhang, Y. Yang, H. Jin, G. Xu, K. Zhang, Proposed combined-cycle power system based on oxygen-blown coal partial gasification, Appl. Energy 102 (2013) 735–745.
[29] O. Govin, V. Diky, G. Kabo, A. Blokhin, Evaluation of the chemical exergy of fuels and petroleum fractions, J. Therm. Anal. Calorim. 62 (1) (2000) 123–133.
[30] E. Biagini, F. Barontini, L. Tognotti, Gasification of agricultural residues in a demonstrative plant: corn cobs, Bioresour. Technol. 173 (2014) 110–116.
[31] Y. Cao, Y. Wang, J.T. Riley, W.-P. Pan, A novel biomass air gasification process for producing tar-free higher heating value fuel gas, Fuel Process. Technol. 87 (4) (2006) 343–353.
[32] A.A.P. Susastriawan, H. Saptoadi, Purnomo, Small-scale downdraft gasifiers for biomass gasification: a review, Renew. Sustain. Energy Rev. 76 (2017) 989–1003.
[33] L. Wu, L. Wang, Y. Wang, X. Hu, C. Dong, Z. Yang, Y. Yang, Component and process based exergy evaluation of a 600MW Coal-fired power plant, Energy Procedia 61 (2014) 2097–2100.
[34] J. Zhen, Exergy Analysis of Supercritical Steam Turbine Thermal System, Shaanxi University of Science and Technology, 2015.
[35] L. Cui, Y. Li, Y. Tang, Y. Shi, Q. Wang, X. Yuan, J. Kellett, Integrated assessment of the environmental and economic effects of an ultra-clean flue gas treatment process in coal-fired power plant, J. Clean. Prod. 199 (2018) 359–368.
[36] P. Córdoba, Status of Flue Gas Desulphurisation (FGD) systems from coal-fired power plants: overview of the physic-chemical control processes of wet limestone FGDs, Fuel 144 (2015) 274–286.
[37] A. Franco, A.R. Diaz, The future challenges for “clean coal technologies”: joining efficiency increase and pollutant emission control, Energy 34 (3) (2009) 348–354.
[38] X.Q. Mao, A. Zeng, T. Hu, Y.K. Xing, J. Zhou, Z.Y. Liu, Co-control of local air pollutants and CO_2 from the Chinese coal-fired power industry, J. Clean. Prod. 67 (2014) 220–227.
[39] Z.Q. Li, F. Wei, Y. Jin, Numerical simulation of pulverized coal combustion and NO formation, Chem. Eng. Sci. 58 (23-24) (2003) 5161–5171.